



Contents lists available at ScienceDirect

Journal of Biomechanics

journal homepage: www.elsevier.com/locate/jbiomech
www.JBiomech.com

Short communication

Probing mechanical properties of fully hydrated gels and biological tissues

Georgios Constantinides^{a,1}, Z. Ilke Kalcioğlu^a, Meredith McFarland^a,
James F. Smith^c, Krystyn J. Van Vliet^{a,b,*}^a Department of Materials Science and Engineering, Massachusetts Institute of Technology, Cambridge, MA 02139, USA^b Department of Biological Engineering, Massachusetts Institute of Technology, Cambridge, MA 02139, USA^c Micro Materials Ltd., Wrexham Technology Park, Wrexham LL13 7YP, UK

ARTICLE INFO

Article history:

Accepted 14 August 2008

Keywords:

Mechanical properties
Indentation
Elasticity
Hydrated tissues
Hydrogels

ABSTRACT

A longstanding challenge in accurate mechanical characterization of engineered and biological tissues is maintenance of both stable sample hydration and high instrument signal resolution. Here, we describe the modification of an instrumented indenter to accommodate nanomechanical characterization of biological and synthetic tissues in liquid media, and demonstrate accurate acquisition of force–displacement data that can be used to extract viscoelastoplastic properties of hydrated gels and tissues. We demonstrate the validity of this approach via elastoplastic analysis of relatively stiff, water-insensitive materials of elastic moduli $E > 1000$ kPa (borosilicate glass and polypropylene), and then consider the viscoelastic response and representative mechanical properties of compliant, synthetic polymer hydrogels (polyacrylamide-based hydrogels of varying mol%–bis crosslinker) and biological tissues (porcine skin and liver) of $E < 500$ kPa. Indentation responses obtained via loading/unloading hystereses and contact creep loading were highly repeatable, and the inferred E were in good agreement with available macroscopic data for all samples. As expected, increased chemical crosslinking of polyacrylamide increased stiffness ($E \leq 40$ kPa) and decreased creep compliance. E of porcine liver (760 kPa) and skin (222 kPa) were also within the range of macroscopic measurements reported for a limited subset of species and disease states. These data show that instrumented indentation of fully immersed samples can be reliably applied for materials spanning several orders of magnitude in stiffness ($E =$ kPa–GPa). These capabilities are particularly important to materials design and characterization of macromolecules, cells, explanted tissues, and synthetic extracellular matrices as a function of spatial position, degree of hydration, or hydrolytic/enzymatic/corrosion reaction times.

© 2008 Elsevier Ltd. All rights reserved.

1. Introduction

It is now appreciated that cell morphology/function can be correlative with the stiffness of biological and synthetic materials to which cells adhere (Discher et al., 2005; Yeung et al., 2005). Although mechanical properties of compliant, hydrated polymers are increasingly inferred from indentation force–depth (P – h) responses acquired via atomic force microscopes (AFMs), (e.g., Ho et al., 2004; Thompson et al., 2005), several aspects of this cantilever-based deformation preclude straightforward, accurate mechanical characterization (e.g., limited maximum force/depth range (~ 100 nN/2 μ m), limited probe materials/geometries, and objective identification of initial contact points). Instrumented indentation employs comparably rigid load frames to impose

normal probe–surface contact that can be mapped rapidly over cm-scale surface areas (Tweedie et al., 2005), surmounting these challenges for imposed forces greater than μ N. With notable exception (Bushby et al., 2004; Carillo et al., 2005; Kaufman et al., 2008), indenters are typically operated in ambient air on dry samples. Given the increasing effort to quantify and mimic the mechanical properties of tissues (Balooch et al., 1998; Ebenstein and Pruitt, 2006), robust mechanical analysis of biological/synthetic polymers in fully hydrated states is required. Here, we demonstrate this experimental capability through modification of an instrumented indentation apparatus, validating accuracy of acquired force–displacement data on water-inert materials and compliant hydrogels, and then applying this approach to biological tissues.

2. Materials and methods

To validate the modified apparatus, several synthetic and biological materials were probed in the fully hydrated, immersed state at 24 °C. Borosilicate glass and polypropylene were obtained from VWR and Aldrich, respectively. Polyacrylamide (PAAm)-based hydrogels (10% bis–tris NovaGel of proprietary composition,

* Corresponding author at: Department of Materials Science and Engineering, Massachusetts Institute of Technology, Room 8-237, 77 Massachusetts Avenue, Cambridge, MA 02139, USA. Tel.: +1 617 253 3315; fax: +1 617 252 8754.

E-mail address: krystyn@mit.edu (K.J. Van Vliet).

¹ Current address: Department of Mechanical Engineering and Materials Science and Engineering, Cyprus University of Technology, Lemesos 3036, Cyprus.

Invitrogen) and freshly synthesized PAAm of $2 \times 2 \times 0.5 \text{ mm}^3$ and varying mol%-bis crosslinker, prepared on amine-derivitized glass slides, were stored in water throughout testing. Porcine tissues (skin and liver) of $5 \times 5 \times 1.5 \text{ mm}^3$ were microtomed and mounted on glass slides with a thin layer of cyanoacrylate. Tissues were stored in phosphate-buffered saline and tested within an hour of mounting/immersion to minimize degradation of structure/mechanical properties.

The instrumented indentation platform modified for liquid-immersed experiments (NanoTest, Micro Materials Ltd.) relies on a vertical pendulum that rotates about a frictionless pivot. This configuration confers horizontal loading, normal to a vertically mounted sample, and has been used widely in mechanical characterization of metal, ceramic, and polymeric surfaces, e.g., Dao et al. (2001) and Tweedie et al. (2007). Force application proceeds via an electromagnetic coil/magnet at the pendulum top, and displacement is acquired via a capacitor positioned behind the indenter (Fig. 1A). Upon calibration of displacement (nm/V), force ($\mu\text{N}/\text{V}$), and frame compliance (nm/ μN) (Van Vliet et al., 2004), the P/h resolutions were $0.1 \mu\text{N}/0.1 \text{ nm}$, respectively. As shown in Fig. 1, the extended, stainless steel indenter mount is immersed within the liquid cell; this cell inclusive of mounted samples is positioned via automated stage displacement. The indenter automatically contacts the sample in two stages: (1) With the pendulum held against a mechanical stop by an arbitrarily low force, the sample stage moves towards the indenter at low velocity until contact displaces the pendulum from its rest position. Displacement is detected at capacitive sensor resolution of $<0.1 \text{ nm}$, upon which stage motion ceases and the indenter falls away from the surface. (2) The specimen retracts a known distance; the indenter is slowly moved into contact at the now-defined measurement plane, at a location laterally displaced from the original site to avoid initial contact damage. The force applied to the indenter at this point is determined from an initial calibration procedure that finds the coil

current required to move the indenter to the measurement plane. Liquids can be added before/after this operation, and exchanged intermittently.

We first validated the accuracy of $P-h$ acquisition and inferred properties of two relatively water-insensitive materials, borosilicate glass (repetitions, $n = 8$) and polypropylene ($n = 8$), using a diamond Berkovich indenter. Trapezoidal loading functions to maximum load P_{max} were used, with dwell and un/loading times of 5 and 10 s, respectively. For glass, $P_{\text{max}} = 100 \text{ mN}$; for polypropylene, P_{max} ranged from 3 to 19 mN in 10 equal intervals ($n = 8$ per interval). We then indented PAAm-based hydrogels ($n = 8$ for each mol% bis) in air and in water, with dwell and un/loading times of 20 and 10 s, respectively, a ruby spherical probe of 1 mm-diameter was chosen to reasonably approximate linear viscoelastic deformation and to induce comparable strains on all samples to $h_{\text{max}} = 1500 \text{ nm}$. Indentation modulus E_r was calculated from the unloading slope dP/dh evaluated at P_{max} and the indenter area function $A_c(h_c)$ obtained through parallel indentations on quartz, according to established analyses for elastoplastic materials (Oliver and Pharr, 1992). E_r of gels (E_{gel}) and tissues (E_s) was corrected for finite sample thickness on a stiff glass substrate ($E_{\text{substrate}} = 69 \text{ GPa}$; $\nu = 0.3$) for the measured ratio of geometrically calculated contact radius a to measured sample thickness t (see Constantinides et al., 2006). For comparison with AFM-enabled indentation of PAAm hydrogels, $P-h$ responses were acquired in an AFM fluid cell (PicoPlus, Agilent) with Si_3N_4 cantilevers of nominal spring constant $k = 0.1 \text{ N/m}$ (Veeco), and E_s calculated as in Thompson et al. (2005).

Using the 1-mm-diameter probe, we also conducted contact creep experiments on PAAm hydrogels and hydrated porcine skin and liver tissues ($n = 5$). Samples were rapidly loaded (1 s) to $P_0 = 200 \mu\text{N}$ (PAAm) or $145 \mu\text{N}$ (tissues); the resulting depth increase $h(t)$ was monitored, respectively, over 30 and 300 s, respectively. Responses were analysed using a linear viscoelastic Kelvin-Voigt

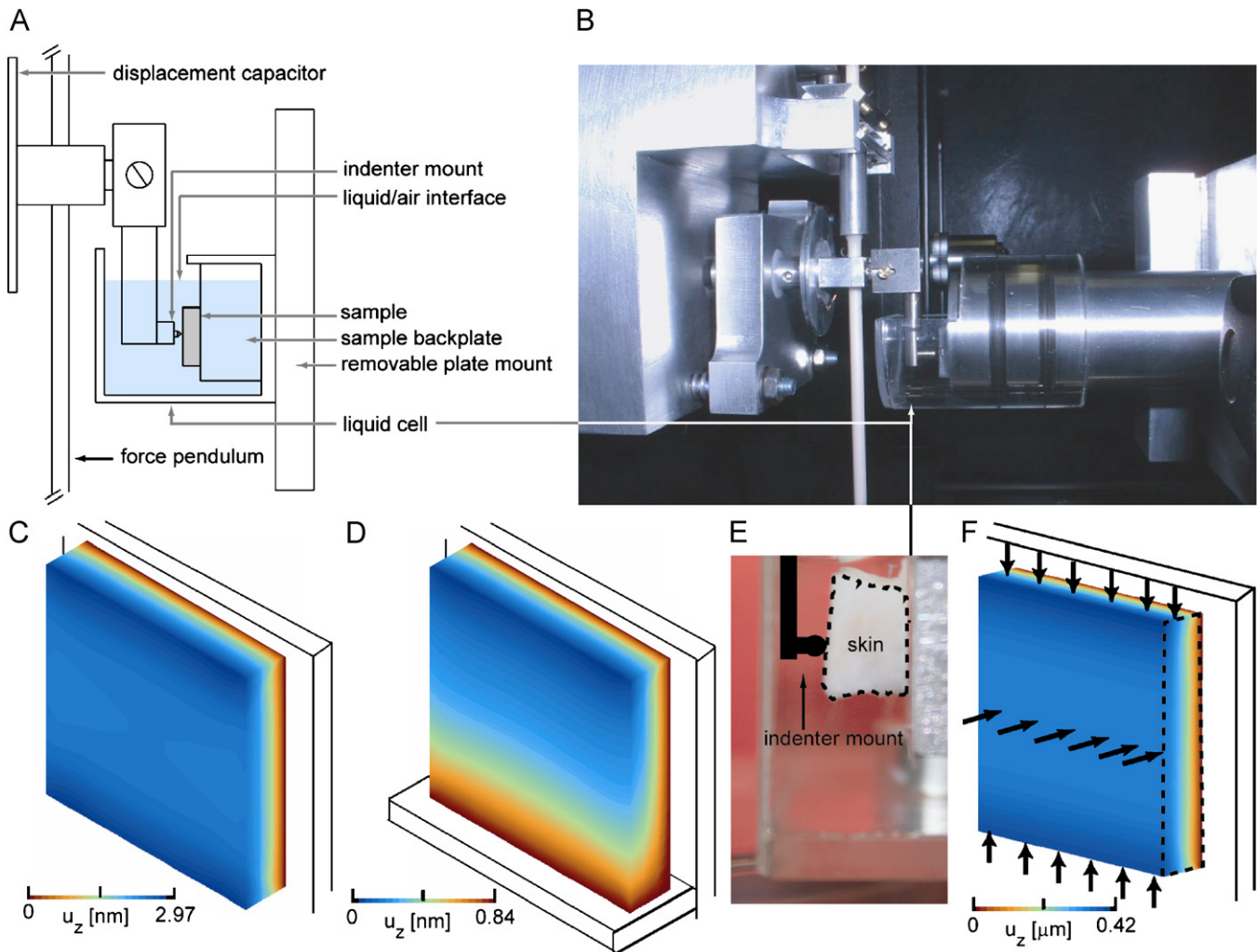


Fig. 1. Schematic diagram (A) and photograph (B) of instrumented indenter apparatus capable of extended nanomechanical experiments in fully immersed environments on hydrated gels and tissues. Finite element analysis of sample surface displacement, assuming a linear elastic material of $E = 1 \text{ MPa}$ and Poisson's ratio $\nu = 0.5$ adhered to a rigid backplate, indicates a $<3 \text{ nm}$ maximum vertical displacement u_z whether the sample is unsupported (C) or supported (D) by a rigid shelf. (E) Submerged porcine skin does not visibly sag after 1 h (dashed). Finite element of model tissue of $E = 20 \text{ kPa}$ in simulated water buoyancy indicates submicron surface displacement (F) and Pa-level-associated stresses (not shown).

model expressed by (Cheng et al., 2005):

$$h^{3/2}(t) = \left(\frac{3}{4} \sqrt{\frac{3P_0^2}{4RE_1^2}} \right) \left(\left(\frac{E_1 + E_2}{E_2} \right) - \left(\frac{E_1}{E_2} \right) e^{-((E_2 t)/3\eta)} \right)$$

3. Results and discussion

As shown in Fig. 1, the horizontal-loading configuration confers significant advantages for indentation in liquids, obviating vertical-loading effects due to variation in buoyancy and surface tension during vertical indenter displacement through liquid. In absolute terms such forces are quite small, but can be significant for the nanoscale forces and/or displacements relevant to compliant hydrogels (Kaufman et al., 2008) or tissues. Vertical sample orientation requires adhesion to a rigid backplate. In the absence of buoyancy, finite element analysis indicates that the free surface of an adhered sample of size $5 \times 5 \times 1 \text{ mm}^3$ and elastic properties comparable to rubber ($E_s = 1 \text{ MPa}$; $\nu = 0.5$) would displace $u_z < 3 \text{ nm}$ whether unsupported (Fig. 1C) or supported by a rigid shelf (Fig. 1D). For samples of identical thickness, u_z increases with decreasing E_s (e.g., $u_z < 0.9 \mu\text{m}$ for $E_s = 20 \text{ kPa}$), but buoyancy of immersed samples (Fig. 1E) further reduces sample surface displacement to $u_z < 0.4 \mu\text{m}$ (Fig. 1F). Associated internal stresses are in the Pa-range and are not expected to significantly affect calculated elastic properties (Bolshakov et al., 1996).

To demonstrate that P - h precision/accuracy was preserved following instrument modifications and introduction of liquids, experiments were conducted on borosilicate glass and polypropylene; neither was expected to absorb/react appreciably with water. Excellent repeatability of borosilicate indentations was observed in water, and P - h responses in air/water were indistinguishable (Fig. 2A). Fig. 2B shows invariance of E_i , extracted from P - h responses of polypropylene in air and in water over a wide range of plastic contact depths h_c (within standard deviation from mean among replicate experiments of $\sim 7\%$ at each h_c). This confirms the absence of mechanically relevant changes in the polypropylene surface and demonstrates reliable data acquisition in liquid. For both materials, we found good agreement between calculated E_s and that reported in the literature (Table 1).

To demonstrate validity on compliant, hydrated materials, experiments were conducted on PAAm gels and porcine tissues. As expected, P - h responses of PAAm-based electrophoresis gels depend strongly on whether the materials were in a dried or fully hydrated state, with excellent repeatability of the hydrated response (Fig. 3A, $n = 5$). Significant increases in penetration depth upon full hydration were correlative with 1000-fold decreases in stiffness ($E_{\text{gel,water}} = 266 \pm 27 \text{ kPa}$; $E_{\text{gel,air}} = 295 \pm 26 \text{ MPa}$). Fig. 3B shows that this approach can also be used to determine E_{gel} as a function of synthesis conditions such as mol%-bisacrylamide crosslinker, commonly employed to tune PAAm-hydrogel stiffness to approximate tissues including fat, brain, and muscle (Yeung et al., 2005). Although rigorous viscoelastoplastic analysis is beyond the scope of this paper (Oyen and Cook, 2003), un/loading rates were optimized to enable reasonable approximation of storage elastic moduli of these polymers according to the Oliver/Pharr method (Cheng and Cheng, 2004). Fig. 3B shows that E_{gel} obtained via indentation in this liquid cell agreed reasonably well with those obtained for gels of similar composition via AFM-enabled indentation by us and by others (Matzelle et al., 2003), and via conventional rheology (Yeung et al., 2005). Since gel architecture and stiffness depend strongly on both mol%-bis and vol%-water during synthesis, better agreement is not expected among disparate hydrogels. Fig. 3B confirms the required sensitivity of this apparatus to measure elastic properties of synthetic gels/biological tissues with stiffness on the order of

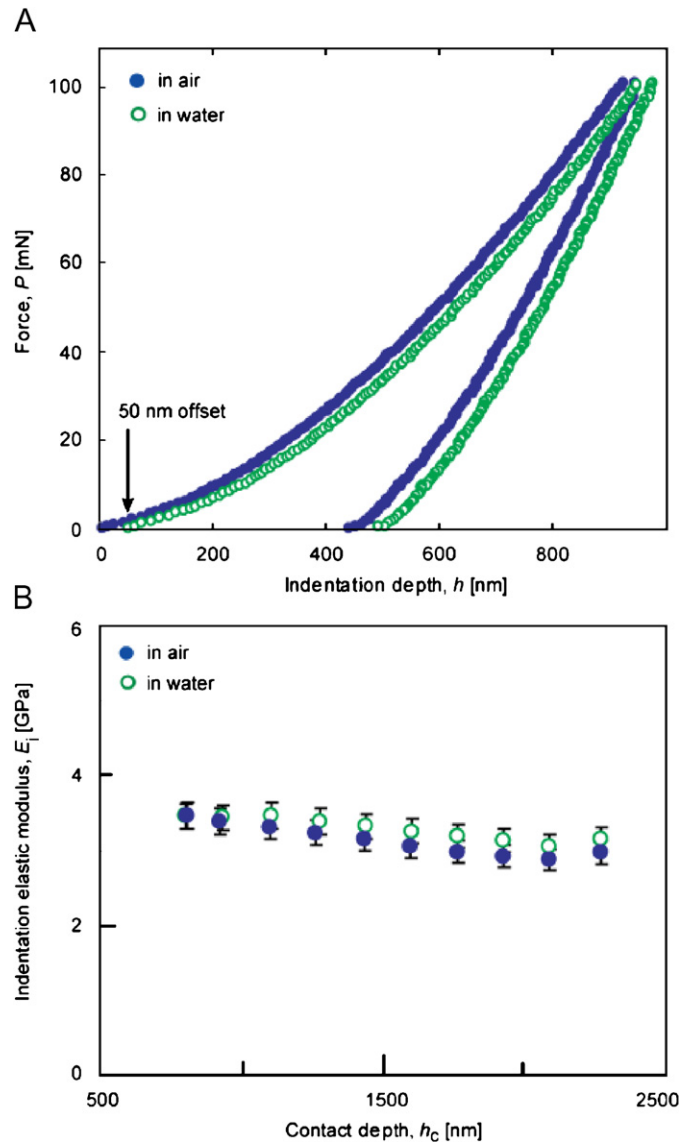


Fig. 2. (A) As expected, response of borosilicate glass under indentation with a sharp Berkovich probe is statistically identical whether acquired in ambient air (●) or fully submerged in water (○); data intentionally offset at $P = 0$ by 50 nm for clarity. Experimental details: Berkovich probe, $n = 5$ for each testing condition, $P_{\text{max}} = 100 \text{ mN}$, $t_{\text{load}} = t_{\text{unload}} = 10 \text{ s}$, $t_{\text{dwell}} = 5 \text{ s}$. (B) Response of bulk polypropylene in air (●) and in water (○) is also unaffected by immersion of the sample in water. Shown here by the invariance of the extracted indentation elastic modulus $E_i = E_i$ over a wide range of contact depths h_c . Error bars represent standard deviation from mean, among eight replicate experiments (see Table 1). Experimental details: Berkovich probe, $n = 8$ for $P_{\text{max}} = 3$ – 19 mN in 10 equal intervals, $t_{\text{load}} = t_{\text{unload}} = 10 \text{ s}$, $t_{\text{dwell}} = 5 \text{ s}$.

Table 1

Elastic moduli (E_s) extracted from indentations in ambient air and fully immersed in water, for polypropylene and borosilicate glass

Sample	Fluid	E_s (GPa)	E_{lit} (GPa)
Polypropylene	Air	2.56 ± 0.21	1.5–3.0
	Water	2.70 ± 0.15	1.5–3.0
Borosilicate glass	Air	67.67 ± 0.99	65–70
	Water	69.83 ± 0.82	65–70

Data represented as mean \pm one standard deviation. These elastic moduli are independent of the extent of hydration, as expected, and in good agreement with the range of elastic moduli widely reported by others (E_{lit}).

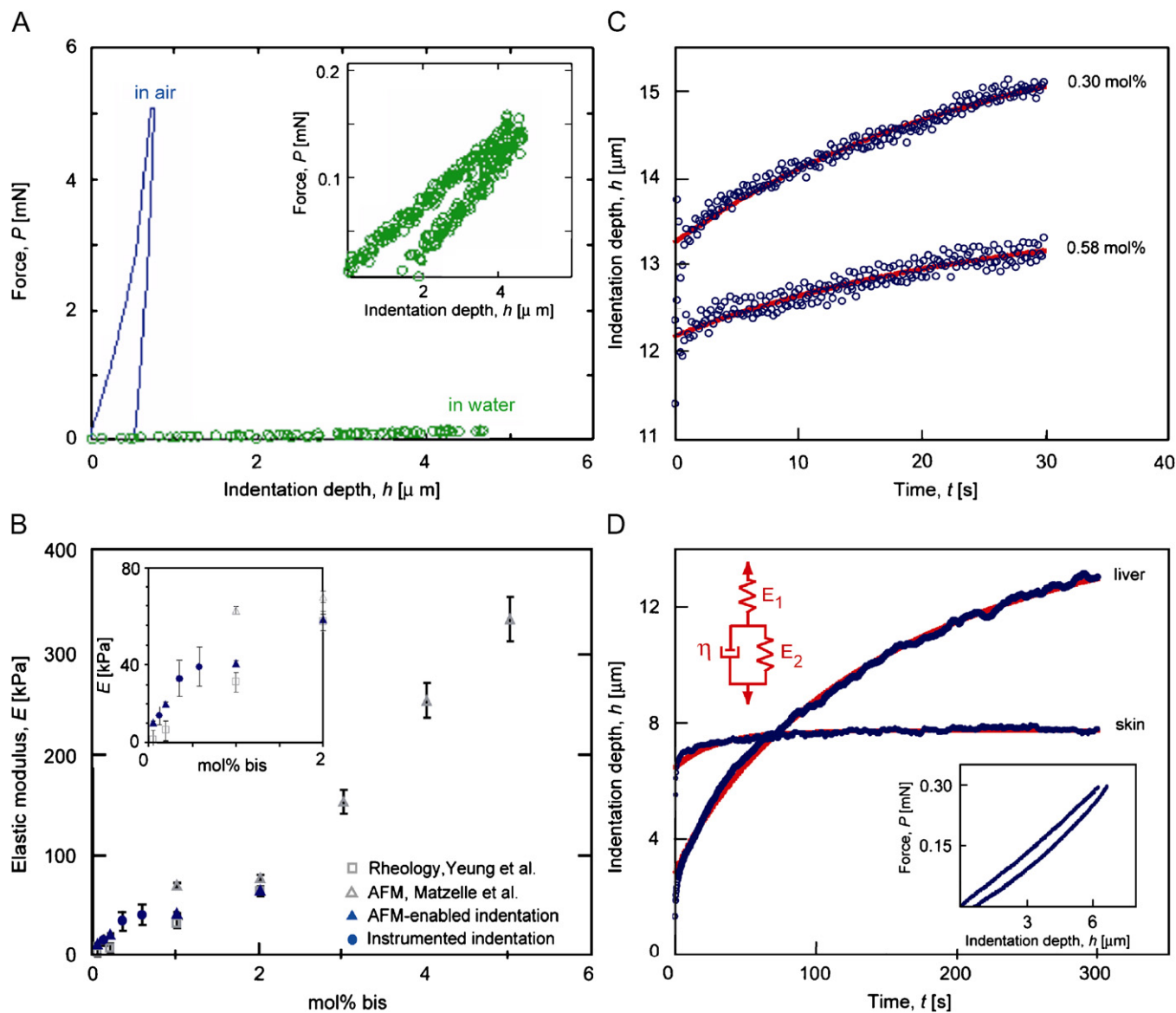


Fig. 3. (A) Response of polyacrylamide gel to spherical indentation in air (blue) and water (green). Inset shows repeatability of five replicate experiments in water. (B) Elastic moduli of PAAm gels as a function of mol% bis measured by instrumented indentation are within the range reported by calibrated AFM-enabled indentation and rheological experiments. The former approach is amenable to rapidly mapping variations in this stiffness over surface areas $> \text{mm}^2$ or as a function of depth $> 1 \mu\text{m}$, and with fewer experimental artifacts as discussed in the text. Error bars represent one standard deviation from mean. (C) Contact creep response of PAAm hydrogels demonstrates increased creep resistance for increased mol%-crosslinker, as expected. (D) Contact creep response of hydrated porcine and skin liver (blue points) at applied load of $145 \mu\text{N}$ fit by Kelvin-Voigt model (red lines). Inset: response of porcine skin to spherical indentation in physiological saline after 1 h immersion shows viscoelastic behavior. These depths probe the mechanical response of the epidermis, which extends 30–140 μm from the free surface (Vardaxis et al., 1997).

~ 10 kPa. This comparison underscores the need for consideration of finite sample thickness when such compliant gels are characterized via indentation: elastic mismatch between the specimen and the underlying, stiffer substrata can incur significant errors in calculated E_s (Constantinides et al., 2006).

As one goal of synthetic hydrogel design is to match tissue stiffness, we also conducted elastic analysis of hydrogels/tissues via contact creep experiments. Reversibility of the un/loading response (Fig. 3D, inset) justified viscoelastic analysis, and the Kelvin-Voigt model reasonably approximated creep responses of PAAm (Fig. 3C) and porcine liver/skin (Fig. 3D). As expected, increased bis-crosslinker from 0.30 to 0.58 mol% decreased creep compliance and increased effective storage moduli $E_1 = E_s$ of PAAm (10 and 12 kPa, respectively). These E_s agree within a factor of 4 with those inferred from elastic unloading (Fig. 1B), with discrepancy attributable in part to significantly different assump-

tions of analytical models used to estimate E_s from creep compliance and elastic unloading, respectively. For liver, the creep response indicates $E_1 = 760$ kPa; $E_2 = 67$ kPa; $\eta = 4.5$ MPa s; and for skin, $E_1 = 222$ kPa; $E_2 = 720$ kPa; $\eta = 7.3$ MPa s. E_s corresponding to this model for liver (760 kPa) and skin (222 kPa) are within the range of reported values ($E_{\text{liver, lit}} = 1 \text{ kPa} - 40 \text{ MPa}$; $E_{\text{skin, lit}} = 300 - 800 \text{ kPa}$) over a range of species, pathologies, and E_s measurement methods (Hollenstein et al., 2006; Yin et al., 2004).

In summary, we have developed and demonstrated an approach to enable nano- to micro-scale indentation of fully immersed, hydrated polymers and tissues that maintains accurate acquisition of high precision force and displacement signals. We anticipate that the platform will enable quantitative studies of tissue mechanics as a function of source, disease state, and exposure to soluble toxins or adjuvants, particularly as a function of submicrometer position within the tissue.

Conflict of interest statement

The authors have no conflict of interest.

Acknowledgements

The authors acknowledge the NSF MRSEC Center for Materials Science and Engineering (KJVV) and REU program (MM), Institute for Soldier Nanotechnologies supported by the US Army Research Office (IZK), and the Arnold & Mabel Beckman Foundation Young Investigator and NSF CAREER Awards (KJVV) for partial funding of this research. We also gratefully acknowledge Mr. J. Choi and Ms. E.B. Walton for synthesis of polyacrylamide gels used in AFM-enabled indentation and instrumented indentation, respectively (Fig. 3B), and Prof. R. Hayward for contribution of well-characterized polyacrylamide gels and helpful discussion of others' analysis of hydrogel mechanical properties.

References

- Balooch, M., et al., 1998. Viscoelastic properties of demineralized human dentin measured in water with atomic force microscope (AFM)-based indentation. *Journal of Biomedical Materials Research* 40, 539.
- Bolshakov, A., Oliver, W.C., Pharr, G.M., 1996. Influences of stress on the measurement of mechanical properties using nanoindentation: Part II. Finite element simulations. *Journal of Materials Research* 11 (3), 760–768.
- Bushby, A.J., Ferguson, V.L., Boyde, A., 2004. Nanoindentation of bone: comparison of specimens tested in liquid and embedded in polymethylmethacrylate. *Journal of Materials Research* 19 (1), 249–259.
- Carillo, F., et al., 2005. Nanoindentation of polydimethylsiloxane elastomers: effect of crosslinking, work of adhesion, and fluid environment on elastic modulus. *Journal of Materials Research* 20, 2820–2830.
- Cheng, Y.T., Cheng, C.M., 2004. Scaling, dimensional analysis, and indentation measurements. *Materials Science and Engineering R* 44, 91.
- Cheng, L., Xia, X., Scriven, L.E., Gerberich, W.W., 2005. Spherical-tip indentation of viscoelastic material. *Mechanics of Materials* 37, 213.
- Constantinides, G., Ravi Chandran, K.S., Ulm, F.-J., Van Vliet, K.J., 2006. Grid indentation analysis of composite microstructures: principles and validation. *Materials Science and Engineering A* 430, 189–202.
- Dao, M., Chollacoop, N., Van Vliet, K.J., Venkatesh, T.A., Suresh, S., 2001. Computational modeling of the forward and reverse problems in instrumented sharp indentation. *Acta Materialia* 49 (19), 3899–3918.
- Discher, D.E., Janmey, P., Wang, Y.L., 2005. Tissue cells feel and respond to the stiffness of their substrate. *Science* 310, 1139–1143.
- Ebenstein, D.M., Pruitt, L.A., 2006. Nanoindentation of biological materials. *NanoToday* 1, 26.
- Ho, S.P., Balooch, M., Goodis, H.E., Marshall, G.W., Marshall, S.J., 2004. Ultrastructure and nanomechanical properties of cementum dentin junction. *Journal of Biomedical Materials Research A* 68 (2), 343–351.
- Hollenstein, M., Nava, A., Valtorta, D., Snedeker, J.G., Mazza, E., 2006. Mechanical characterization of the liver capsule and parenchyma. *Lectures Notes in Computer Science* 4072, 150–158.
- Kaufman, J.D., Miller, G.J., Morgan, E.F., Klapperich, C.M., 2008. Time-dependent mechanical characterization of poly (2-hydroxyethyl methacrylate) hydrogels using nanoindentation and unconfined compression. *Journal of Materials Research* 23 (5), 1472–1481.
- Matzelle, T.R., Geuskens, G., Kruse, N., 2003. Elastic properties of poly (N-isopropylacrylamide) and poly(acrylamide) hydrogels studied by scanning force microscopy. *Macromolecules* 36, 2926–2931.
- Oliver, W.C., Pharr, G.M., 1992. An improved technique for determining hardness and elastic-modulus using load and displacement sensing indentation experiments. *Journal of Materials Research* 7, 1564.
- Oyen, M.L., Cook, R.F., 2003. Load–displacement behavior during sharp indentation of viscous–elastic–plastic materials. *Journal of Materials Research* 18, 139–150.
- Thompson, M.T., Berg, M.C., Tobias, I.S., Rubner, M.F., Van Vliet, K.J., 2005. Tuning compliance of nanoscale polyelectrolyte multilayers to modulate cell adhesion. *Biomaterials* 26 (34), 6836–6845.
- Tweedie, C.A., Anderson, D.G., Langer, R., Van Vliet, K.J., 2005. Combinatorial material mechanics: high-throughput polymer synthesis and nanomechanical screening. *Advanced Materials* 17 (21), 2599–2603.
- Tweedie, C.A., et al., 2007. Enhanced stiffness of amorphous polymer surfaces under confinement of localized contact loads. *Advanced Materials* 19 (18), 2540–2545.
- Van Vliet, K.J., Prchlik, L., Smith, J.F., 2004. Direct measurement of indentation frame compliance. *Journal of Materials Research* 19 (1), 325–331.
- Vardaxis, N.J., Brans, T.A., Boon, M.E., Kreis, R.W., Mars, L.M., 1997. Confocal laser microscopy of porcine skin: implications for wound healing studies. *Journal of Anatomy* 190, 601–611.
- Yeung, T., et al., 2005. Effects of substrate stiffness on cell morphology, cytoskeletal structure, and adhesion. *Cell Motility and the Cytoskeleton* 60, 24–34.
- Yin, H.M., Sun, L.Z., Wang, G.a., Vannier, M.W., 2004. Modeling of elastic modulus evolution of cirrhotic human liver. *IEEE Transactions on Biomedical Engineering* 51, 10–18.